Received: 24 February 2022 | Accepted: 17 June 2022

DOI: 10.1002/bab.2380

ORIGINAL ARTICLE

WILEY

Cardiovascular biomarker troponin I biosensor: Aptamer-gold-antibody hybrid on a metal oxide surface

Hu hui[1] | **Subash C. B. Gopinath**[2,3] | **Zool H. Ismail**[4] | **Yeng Chen**[5] | **K. Pandian**[6] | **Palaniyandi Velusamy**[7]

[1]Department of Geriatrics, Luzhou People's Hospital, Luzhou, China

[2]Institute of Nano Electronic Engineering, Universiti Malaysia Perlis (UniMAP), Kangar, Perlis, 01000, Malaysia

[3]Faculty of Chemical Engineering Technology, Universiti Malaysia Perlis (UniMAP), Arau, Perlis, 02600, Malaysia

[4]Centre for Artificial Intelligence and Robotics, Universiti Teknologi Malaysia, Kuala Lumpur, Malaysia

[5]Department of Oral & Craniofacial Sciences, Faculty of Dentistry, University of Malaya, Kuala Lumpur, Malaysia

[6]Department of Inorganic Chemistry, University of Madras, Guindy Campus, Chennai, India

[7]Research and Development Wing, Sree Balaji Medical College and Hospital (SBMCH), Bharath Institute of Higher Education and Research (BIHER), Chromepet, Chennai, Tamil Nadu, 600044, India

Correspondence
Subash C. B. Gopinath, Institute of Nano Electronic Engineering, Universiti Malaysia Perlis (UniMAP), 01000 Kangar, Malaysia.
Email: subash@unimap.edu.my

Abstract

Myocardial infarction (MI) is highly related to cardiac arrest leading to death and organ damage. Radiological techniques and electrocardiography have been used as preliminary tests to diagnose MI; however, these techniques are not sensitive enough for early-stage detection. A blood biomarker-based diagnosis is an immediate solution, and due to the high correlation of troponin with MI, it has been considered to be a gold-standard biomarker. In the present research, the cardiac biomarker troponin I (cTnI) was detected on an interdigitated electrode sensor with various surface interfaces. To detect cTnI, a capture aptamer-conjugated gold nanoparticle probe and detection antibody probe were utilized and compared through an alternating sandwich pattern. The surface metal oxide morphology of the developed sensor was proven by microscopic assessments. The limit of detection with the aptamer-gold-cTnI-antibody sandwich pattern was 100 aM, while it was 1 fM with antibody-gold-cTnI-aptamer, representing 10-fold differences. Further, the high performance of the sensor was confirmed by selective cTnI determination in serum, exhibiting superior non-fouling. These methods of determination provide options for generating novel assays for diagnosing MI.

KEYWORDS

aptasensor, cardiovascular disease, immunosensor, interdigitated electrode, troponin biomarker

1 | INTRODUCTION

Cardiovascular disease (CVD) is reported as a major cause of death worldwide,[1,2] and myocardial infarction (MI) is the most dangerous occurrence among CVDs, causing low recovery and high mortality rates. MI occurs when the heart muscle faces unusual blood flow in the artery.[3] The affected patient should be treated within an hour to obtain the highest recovery. Late identification and treatment cause organ damage and lead to death, and rapid identification of MI is mandatory to save the patient's life.[4] Various blood-based biomarkers, including creatine

Abbreviations: CDI, 1,1′-carbonyldiimidazole; cTnI, cardiac biomarker troponin I; CVD, cardiovascular disease; GNP, gold nanoparticle; IDE, interdigitated electrode; MI, myocardial infarction; RT, room temperature; SiO_2, silicon dioxide; UV, ultraviolet.

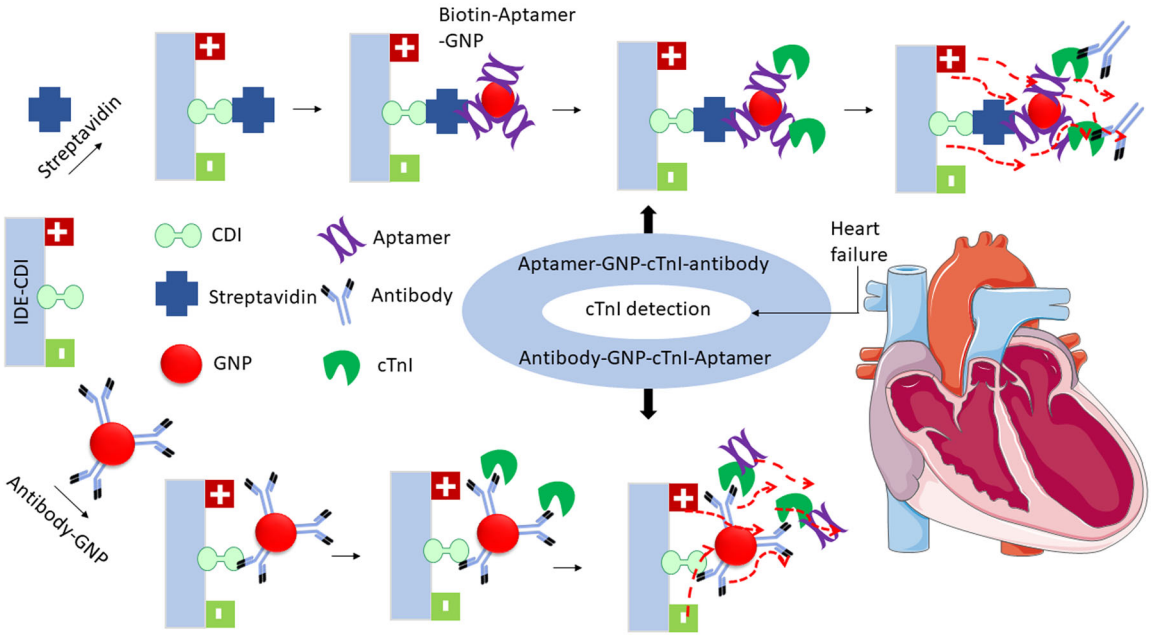

FIGURE 1 Representation of the detection of cTnI by antibody-cTnI-aptamer and aptamer-cTnI-antibody patterns on an IDE sensing surface. The aptamer/antibody was immobilized on the IDE surface through a CDI chemical linker, and cTnI was detected. The antibody/aptamer was conjugated with gold nanoparticles to improve immobilization and detection. The mechanism of the dipole moment on the molecule attached surface is shown by broken red arrows.

kinase, myoglobin, MB isozymes, troponins C, I, and T, have been found to be suitable for diagnosing MI.[5,6] Among them, troponin was proven to be an efficient biomarker, and cardiac troponin I (cTnI) is a unique protein in the muscle cells of the heart that has a high correlation with MI and serves as an efficient biomarker to detect MI.[7–9] This experiment is mainly focused on detecting and quantifying cTnI with its specific binding aptamer and antibody probes on an interdigitated electrode (IDE) sensor. The IDE shown in this study has uniformly arranged finger and gap regions, which will influence the current change upon molecular attachment or in the presence of electrolytes. The system operates at a low-voltage flow and displays changes upon biomolecular interactions on the surface due to the dipole moment (Figure 1; red arrows). The identification of blood biomarkers with a suitable probe is necessary to improve the detection strategy. In general, proteins, DNA, antibodies, RNA, and peptides are utilized as probes to diagnose various diseases.[10–13] Among them, antibodies have been well suited in biosensors and utilized to detect various targets. Another probe, called an aptamer, is a kind of antibody, and either RNA or DNA molecules as aptamers have been created from a randomized library of DNA by three major steps, namely, binding of the target to a molecule, separation of the bound molecule and amplification of the bound molecule.[14] Since the generated aptamers have high specificity and binding affinity with the target, the application of aptamers is widespread in different fields, particularly for disease diagnosis.[15–17] Moreover, due to the specific binding of the aptamer with a few bases on its target, it can discriminate closely related biomolecules. Aptamers produced against influenza could discriminate the subtypes of influenza viral strains. Since aptamers and antibodies have higher possibilities of acquiring different binding sites with the target, the present research utilized both aptamers and antibodies to create different surface interfaces by sandwich patterns for the detection of cTnI. Two different strategies, namely, aptamer-cTnI-antibody and antibody-cTnI-aptamer, were evaluated on the IDE metal oxide surface to evaluate the level of cTnI.

Nanomaterials have been widely accepted to improve biomolecule detection in several ways.[18–24] A broad range of materials have been prepared at the nanoscale level and conjugated with biomolecules to make them more stable during immobilization on the sensing surface.[25–28] Among several available metals, gold is one of the most excellent and well-accepted materials in the biosensor field due to its unique optical properties. Various sensors, including Raman spectroscopy, surface plasmon resonance

spectroscopy, waveguide-mode sensing, and colorimetry, utilize gold particles to improve detection. The current research study used a conjugated antibody/aptamer on GNPs for efficient immobilization on a metal oxide to detect cTnI. It was expected that a higher number of probes can be attached to sensor surfaces to detect the target molecule with a lower level and display massive charge differences. This study involves two different biological probes and two potential nanomaterials as metals. Metal oxide on the sensing surface enhances the surface chemistry to capture a higher number of primary probes, and the second metal (gold) increases the surface area to immobilize a greater number of detection probes. These dual combinations were implemented by a sandwich pattern using both probes either as capture and detection molecules and vice versa. With these different assemblies on the sensing surface, the optimal and best strategy has been found for sensing cTnI.

2 | MATERIALS AND METHODS

2.1 | Chemicals and biomolecules

Cardiac troponin (cTnI), cardiac troponin T, anti-cTnI, 1,1′-carbonyldiimidazole (CDI), phosphate-buffered saline (PBS), human serum, and gold nanoparticles were purchased from Sigma–Aldrich (USA). Ethanolamine was acquired from Fisher Scientific (UK). The SH-aptamer for cTnI was chemically synthesized and received from a local supplier. The complete aptamer sequence (5′-biotin-CGTGCAGTACGCCAACCTTTCTCATGCGCTGCCCCTC TTA-3′) was obtained from Jo et al.[29] The surface morphology of the fabricated IDE was observed by 3D nanoprofilometry (3D-view) and scanning electron microscopy.

2.2 | Interdigitated sensing metal oxide surface fabrication

The sensor metal oxide surface with an IDE was fabricated by following a previous report of the traditional wet-etching process.[30,31] First, a silica substrate was washed with recommended solutions (RCA2 and RCA1) to clean the unnecessary particles. Then, thermal oxidation was carried out for 60 min (500°C) to create a silicon dioxide (SiO_2) layer. Next, aluminium (Al) was used to coat the Al layer on SiO_2 by utilizing a thermal evaporator. The pattern of the electrode was deposited on Al by the following photolithography steps. Then, the IDE pattern was transferred to the surface by exposure to ultraviolet (UV) light. The unexposed place was eliminated by a photoresist developer. Then, IDE was hard-baked (110°C) for 60 s to remove the moisture on the surface. Finally, the area without Al was etched with an etchant solution (Figure 2). The prepared IDE was cleaned with acetone and distilled water. The morphology of IDE was determined by microscopic assessments (high-power microscopy and 3D nanoprofilometry) as recommended previously.[32,33]

2.3 | Preparation of GNP–antibody and GNP–aptamer

To attach the antibody to GNPs, the as-received gold nanoparticles were linked with 16-mercaptoundecanoic acid, and the antibody was mixed with GNPs. Prior to mixing, the linked GNPs were centrifuged to eliminate excess 16-MDA and then activated and stabilized by 50 mM NHS and 200 mM EDC at a ratio of 1:1 for 10 min. The conjugated antibodies on the GNPs were recovered by centrifugation and washed many times with distilled water to eliminate the excess molecules. The aptamer was conjugated with the GNPs through a thiol linker. Then, 1 μM aptamer was mixed with GNPs (10 μL) and maintained at room temperature (RT; 30 min). The conjugated aptamer-GNPs were recovered by centrifugation at a speed of 10,000 *g* (10 min). Then, they were washed five times with distilled water by centrifugation and stored at 4°C. All experiments were performed under the optimized vital factors at room temperature. For GNP and aptamer/antibody conjugation, as-received GNP (one optical density) was added as 1:10 by keeping the desired final concentration of biomolecules. Even though the incubation of these conjugates attained saturation at 20 min, it was prolonged for 30 min to attain a maximum attachment of aptamer/antibody on the GNP.

2.4 | GNP-aptamer/antibody immobilization for metal oxide surface interfaces

cTnI was detected by the aptamer–GNP and antibody–gold nanoparticle conjugates on the metal oxide IDE. For that process, these conjugates were attached to IDE through a CDI chemical linker. In both cases, the linker CDI was used to create the chemical bond between the substrate and biomolecule. To do so, CDI was initially diluted in 30% ethanol at a concentration of 0.5 M and added to the metal oxide IDE sensor surface for 1 h (RT). The unbound CDI was eliminated by PBS buffer and used to immobilize

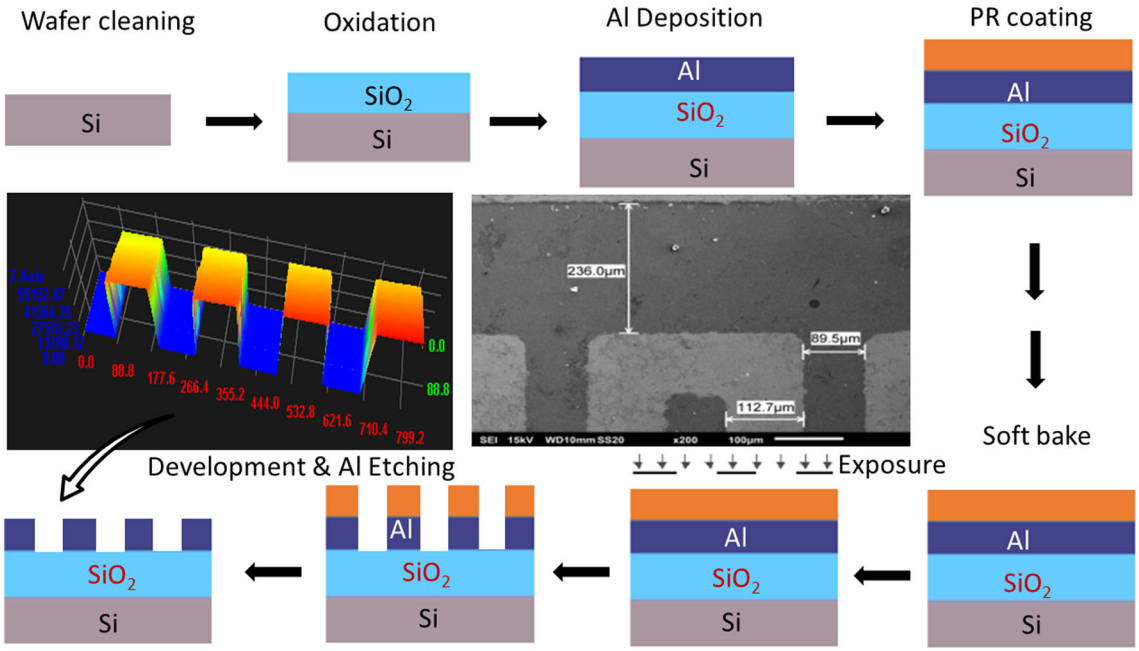

FIGURE 2 Fabrication process of the IDE. Different steps involved in the process are explained. Figure insets are the surface profile by 3D nanoprofilometry (3D-view) and scanning electron microscope images.

the aptamer–gold nanoparticle (GNP–aptamer) and antibody–gold nanoparticle (GNP–antibody) conjugates. To immobilize the aptamer, a biotin–streptavidin strategy was followed. Briefly, 200 nM streptavidin was dropped onto the CDI-attached surfaces and maintained at RT for 1 h. The free CDI surfaces were covered by ethanolamine. Finally, a biotinylated GNP-aptamer (1 μM) was added to the streptavidin-covered IDE. In the case of the antibody–gold nanoparticle conjugate, this complex at a concentration of 200 nM was dropped onto a CDI-attached surface and maintained for 1 h (RT). Then, the excess CDI surfaces were covered with an ethanolamine solution (1 M). These GNP–aptamer and GNP–antibody immobilized sensor surfaces were used to identify cTnI, and the detection performance was compared. The current levels were recorded after each immobilization. All steps were conducted under wet conditions, and washings were performed between each immobilization process.

2.5 | Detection of cTnI on GNP–aptamer/antibody immobilized metal oxide surface interfaces

cTnI was quantified on ethanolamine-blocked GNP–antibody and GNP–aptamer immobilized surfaces. cTnI at a concentration of 100 pM was allowed to interact separately on the GNP—aptamer- and GNP–antibody-modified electrodes. After washing the surface with PBS, the current (before and after interaction with cTnI) was recorded to test the affinity of cTnI to the aptamer and antibody. Unless otherwise stated, all biomolecular modifications and interaction steps were performed under wet conditions with washing between each step. The obtained values were the averages of replicates.

2.6 | Limit of cTnI detection on aptamer- and antibody-modified metal oxide electrodes

The detection limit of cTnI by its antibody and aptamer was calculated by interaction with cTnI concentrations from the lowest attomolar (100 aM) to picomolar (100 pM) levels. The prepared solutions were dropped individually on the GNP–antibody- and GNP–aptamer-modified surfaces. After the washing steps, the current changes were recorded, and the differences were plotted in Excel to estimate the detection limit. The limit of detection (LOD) was considered the lowest concentration of an analyte on the calibration line at low concentrations against the background signal (S/N = 3:1; LOD = standard deviation of the baseline + 3σ).

2.7 | Sandwich patterns of the antibody-cTnI-aptamer and aptamer-cTnI-antibody

To enhance the detection of cTnI, antibody-cTnI-aptamer and aptamer-cTnI-antibody strategies were carried out on metal oxide IDE sensor surfaces. For the antibody-cTnI-aptamer sandwich, 1 μM aptamer was dropped individually onto GNP-antibody-cTnI (from 100 aM to 100 pM) immobilized metal oxide IDE surfaces and maintained for 30 min. After washing, the current changes were noted and compared. In the aptamer-cTnI-antibody sandwich, 200 nM antibody was dropped individually onto GNP-aptamer-cTnI (from 100 aM to 100 pM) immobilized IDE surfaces and maintained for 30 min. The current levels were noted for comparison.

2.8 | Selective and specific detection of cTnI on aptamer- and antibody-immobilized metal oxide surface interfaces

Three control experiments with different biomolecules were used to confirm the selective detection of cTnI. In the case of cTnI and aptamer detection, the control experiments were analyzed with (i) a complementary sequence of the aptamer, (ii) the interaction with cTnT, and (iii) no aptamer. Similarly, for the cTnI and antibody interactions, the control experiments were carried out with (i) nonimmune antibody, (ii) interaction with troponin T, and (iii) no antibody. The results of these control experiments were compared with the specific detection of cTnI with its aptamer and antibody. Further, the specific detection of cTnI was carried out by spiking cTnT in a 1:100 dilution of human serum. Other experimental setups were established as described above. Unless otherwise stated, 10 mM PBS (pH 7.4) was used to maintain the conditions for biomolecular interaction, and the same buffer was used to maintain the wet sensing surface during measurements. A thorough washing was performed between each surface modification or interaction by this buffer using 10 reaction volumes. Current–volt measurements were from 0 to 2 V at 0.1 V interval by a picoammeter, and the obtained values were averaged from three independent experiments.

3 | RESULTS AND DISCUSSION

MI, also called a "heart attack," is caused by the death of heart muscle due to the prolonged lack of oxygen supply. Rapid identification of MI is mandatory for intervention and treatment of mortality and morbidity.[34] The present research was aimed to detect the cardiac biomarker troponin I (cTnI) via interactions with its antibody and aptamer on an IDE electrochemical sensor. Figure 1 depicts the schematic explanation of cTnI identification by using aptamer-cTnI-antibody or antibody-cTnI-aptamer sandwich patterns on the metal oxide IDE surface. Initially, the surface profile of the IDE was observed by 3D nanoprofilometry and scanning electron microscopy, and the observed image indicated that the electrodes were properly fabricated, forming uniformly arranged gaps and fingers on the surface (Figure 2; inset). The IDE utilized in this study was originally designed by AutoCAD software with the desired dimensions as follows: length, 9000 μm; diameter, 3500 μm; two probing points of 1000 μm square and gap and finger regions (18 pairs) with a 5-μm thickness. The gap regions were designed as 90 μm, and they formed fingers of 110 μm. Aptamer/antibody-conjugated GNPs were attached to the IDE by using a CDI chemical linker, and cTnI was detected. To immobilize the aptamer, a strategy taking advantage of the strong binding affinity of biotin–streptavidin was followed. Streptavidin was chemically immobilized on the metal oxide IDE sensor surface, and then the biotinylated aptamer interacted with it. This method of immobilization enhanced the number of aptamers bound on the sensing surface. Various sensing surfaces have proven the efficient detection of biomolecules through this method of immobilization.[35] On the GNP-aptamer-modified surface, cTnI was detected and sandwiched by its specific antibody. Similarly, chemically immobilized GNP antibody interacted with cTnI and sandwiched with the aptamer. Herein, these two methods of determination were compared to improve the efficiency of cTnI detection.

3.1 | Comparison of aptamer and antibody modification on the metal oxide surface

GNP–aptamer and GNP–antibody immobilization on the IDE sensor was compared. Figure 3A explains the process of GNP–antibody immobilization on the IDE sensor through the CDI linker. As indicated in Figure 3A, the bare surface current level was 9.36 nA, and upon adding CDI the value was increased to 405 nA. This current change attests to the attachment of CDI on the metal oxide surface. Further, the GNP antibody was added, and the current level was changed to 856 nA, representing a difference of ~451 nA. Finally, when ethanolamine was dropped, the response of the current was enhanced to 1080 nA. In the case of GNP–aptamer immobilization, after adding

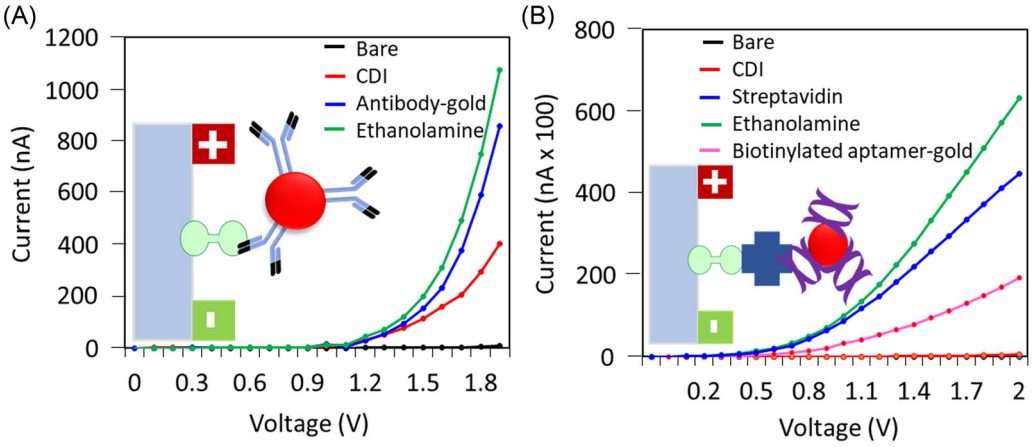

FIGURE 3 (A) Antibody-gold nanoparticle immobilization on the IDE sensor; 200 nM antibody was immobilized on the IDE sensor through a CDI chemical linker, and the surface was blocked by ethanolamine. (B) Aptamer-gold nanoparticle immobilization on the IDE sensor; 200 nM streptavidin was immobilized on the IDE sensor through a CDI chemical linker, and then, the surface was blocked by ethanolamine. On the surface, the biotinylated aptamer was allowed to interact. The current clearly changed after each immobilization step. Figure insets display diagrammatic representation

streptavidin, the current increased from 533 to 44,700 nA. The difference in current was noted to be 446 nA. After the addition of ethanolamine, the current was enhanced further to 63,200 nA. Finally, after the biotinylated GNP aptamer was added, the current changed to 192 nA, and the difference in current was found to be 62,900 nA. Compared with GNP–antibody immobilization, GNP–aptamer immobilization shows larger changes in current due to the differences in charge. Stronger binding of biotin with streptavidin enhanced the interaction of biotinylated aptamers with streptavidin (Figure 3B).

3.2 | Comparative detection of cTnI by aptamer and antibody on metal oxide surface interfaces

On the GNP–aptamer and GNP–antibody surfaces, 100 pM cTnI was added, and the interaction of cTnI with its aptamer and antibody was compared. As seen in Figure 4A, the ethanolamine-blocked surface displays a current level from 1080 to 77.1 nA, representing a difference of 19,700 nA. The current changes confirmed the binding of the antibody with cTnI. Similarly, for the interaction of the aptamer and cTnI, the aptamer-modified surface indicates a current level of 19,200 nA; after the addition of cTnI, the current level increased to 63,200 nA, and the change in current was 44,000 nA. (Figure 4B). This change is ~2 times higher than that with cTnI detection by the antibody. This result might be due to the strong binding of the aptamer with cTnI, and the higher number of immobilized aptamers that interacted with more cTnI. Further, the aptamer was conjugated with GNP, displaying a larger response on the IDE surface and attracting more cTnI. The inset of Figure 4B shows the GNP–aptamer attachment on the metal oxide IDE surface as observed by scanning electron microscopy.

3.3 | Comparison of the detection limit of cTnI by GNP–aptamer and GNP–antibody

To calculate the cTnI detection limit by the aptamer and antibody, cTnI concentrations from 100 aM to 100 pM were placed individually on GNP–aptamer- and GNP–antibody-modified surfaces and the current changes were recorded for comparison. Figure 5A shows the data for different concentrations of cTnI interacting with its antibody. As shown in the figure, when 100 aM cTnI interacted, no significant difference in current was noted after ethanolamine blocking. Then, enhancing the concentration to 1 fM decreased the current level from 1520 to 932 nA. Further, when the cTnI concentration was increased to 0.01, 0.1, 1, and 10 pM, the current level decreased gradually to 40.8, 22.6, 14.3, and 77.1 nA, respectively. The results indicated a clear dose dependence of cTnI with its antibody from 1 fM cTnI. A similar titration was performed on the aptamer-immobilized surface. As indicated in Figure 5B, the aptamer-modified surface displays a current of 19,200 nA; after the addition of 100 aM cTnI, the current changed to 45,700 nA, and the difference was found to be 26,500 nA. This result clearly shows the detection of 100 aM cTnI on the aptamer-attached surface, while it could not be detected on the antibody surface. With further increases in the cTnI concentration on the aptamer surface to 0.001, 0.01, 0.1, 1, and 10 pM, the current levels decreased

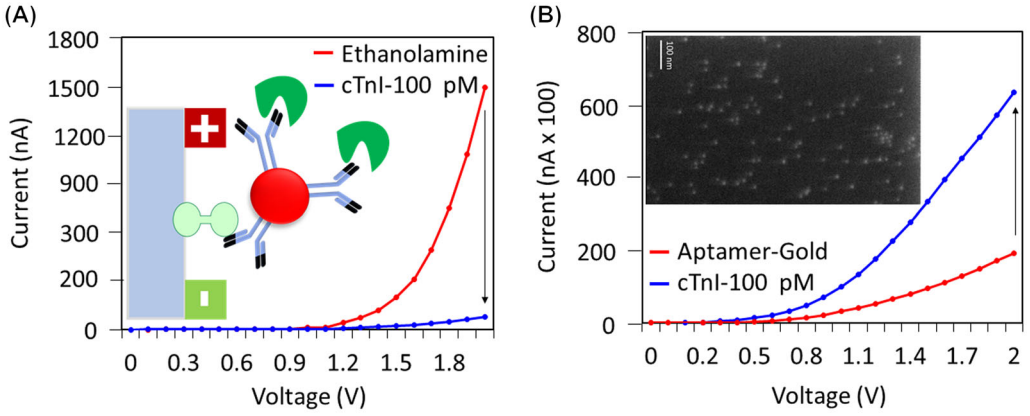

FIGURE 4 cTnI detection on the (A) antibody-modified surface and (B) aptamer-modified surface; 100 pM cTnI was used. With the aptamer, larger current changes were noticed than with the antibody. Figure insets display the diagram and gold nanoparticle attachment on the surface as observed by scanning electron microscopy.

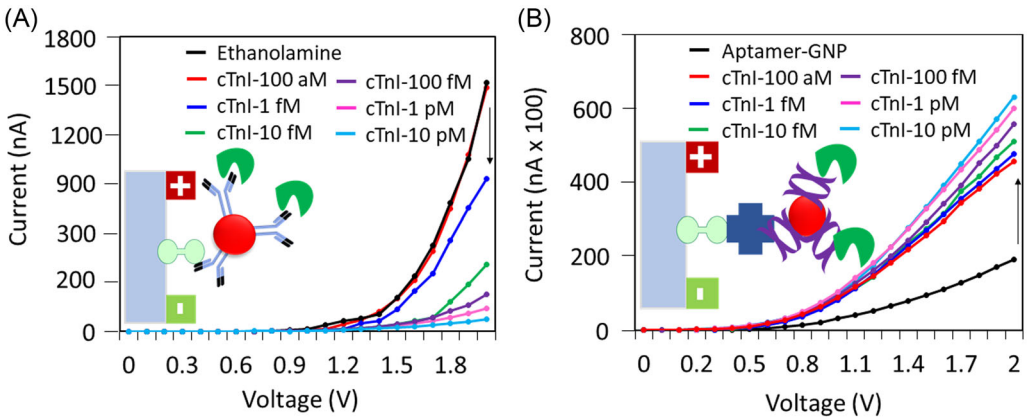

FIGURE 5 Detection limit of cTnI on the (A) antibody-modified surface and (B) aptamer-modified surface. On the antibody-modified surface, from 1 fM cTnI, a clear change in current was noticed, while on the aptamer-modified surface, the change in current was detected from 100 aM cTnI. Figure insets display diagrammatic representation

gradually to 47.7, 50.9, 55.8, 60.1, and 63.2 nA, respectively. At all cTnI concentrations, the aptamer surface shows higher changes in current than the antibody surfaces.

3.4 | Comparison of sandwich patterns of antibody-cTnI-aptamer and aptamer-cTnI-antibody

To improve cTnI detection, the antibody-cTnI-aptamer and aptamer-cTnI-antibody sandwich patterns were evaluated on a metal oxide IDE sensing surface. Figure 6A shows the results obtained from the sandwich pattern of GNP-antibody-cTnI-aptamer. The aptamer was dropped on GNP-antibody-cTnI (from 100 aM to 100 pM) surfaces, and the current variations were noted. It was found that on the 100 aM cTnI surface, there was no significant change after adding the aptamer. This result might be due to decreased or no cTnI interaction on the sensing surface. Further, with higher concentrations of cTnI (0.001, 0.01, 0.1, 1, and 10 pM), clear current changes of 1030, 557, 553, 455, and 647 nA, respectively) were observed on the aptamer-immobilized surfaces (Figure 6B). Based on this result, it is concluded that after sandwiching by the aptamer, there is an increase in the current at lower cTnI concentrations; however, a similar detection is retained. Similarly, 200 nM antibody was dropped on GNP-aptamer-cTnI (from 100 aM to 100 pM) surfaces, and current variations were noted. From 100 aM to 100 pM cTnI, the current levels all increased after sandwiching with the antibody was performed (Figure 6C). As shown in Figure 6D, at higher concentrations of cTnI, a clear decrease in current was seen upon adding the antibody, indicating clear detection by the aptamer-cTnI-antibody sandwich. The primary difference originates from the number of molecules interacting with the target, which is

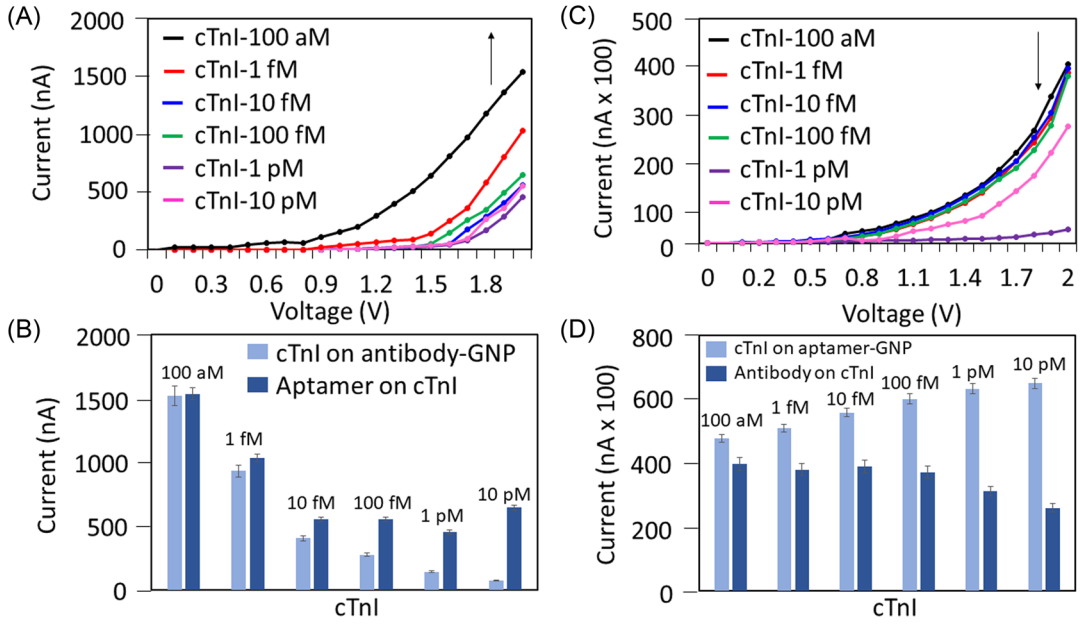

FIGURE 6 (A) Detection of the antibody-cTnI-aptamer sandwich pattern. The aptamer was dropped on antibody-cTnI (from 100 aM to 100 pM)-modified surfaces. From 1 fM cTnI, current changes were noticed. (B) Comparison of current changes by interacting cTnI with the antibody and aptamer. (C) Detection of the aptamer-cTnI-antibody sandwich pattern. The antibody was dropped on aptamer-cTnI (from 100 aM to 100 pM)-modified surfaces. From 100 aM cTnI, current changes were noticed. (D) Comparison of current changes by interacting cTnI with the aptamer and antibody. Error bars are based on average values with replicates.

determined by the affinity of the probe (aptamer/antibody) and the size. If the capture molecule has a high affinity for the target, then more target molecules will interact. Usually, aptamers have been found to exhibit a higher affinity and smaller size than antibodies. For the same reasons, the current study shows differences between the antibody-cTnI-aptamer and aptamer-cTnI-antibody sandwich patterns. In this work, the aptamer played an efficient role as the capture probe and attracted a higher level of cTnI molecules, leading to improved detection.

3.5 | Linear regression: Sensitivity analysis

Correlations between variables were graphically analyzed using the slope of the regression line, along with the covariance of the model (R^2) and the standardized correlation coefficient. With aptamer-cTnI and antibody-cTnI, the estimated R^2 values were 0.9922 and 0.9002, respectively, whereas the antibody-cTnI-aptamer and aptamer-cTnI-antibody sandwich patterns produced the same R^2 value of 0.9732. The LOD was analyzed by calculating the standard deviation of the baseline + 3σ. The detection limit with the aptamer-gold-cTnI-antibody assembly was 100 aM, while it was 1 fM with the antibody-gold-cTnI-aptamer assembly (Figures 7A and 8B).

3.6 | Control experiments for specific detection of cTnI

Three control experiments were performed to check the specific detection of cTnI. On the surface with the antibody as the probe, the controls were nonimmune antibody, troponin T, and no antibody. Based on the obtained results, these surfaces did not indicate any particular current changes compared with that for the specific interaction (Figure 8A). Similarly, on the streptavidin-biotinylated aptamer-modified surface, the controls were complementary aptamer sequences, troponin T, and no aptamer. As in the above case, the controls did not exhibit any significant current increase compared with that for the specific detection experiment (Figure 8B). These results indicate the specific detection of cTnI on the GNP–aptamer- and GNP–antibody-modified metal oxide IDE surfaces. Further, for applications with clinical samples, cTnI was spiked in diluted human serum. As shown in Figure 9, spiking cTnT in human serum did not significantly influence the current response at all cTnI concentrations compared to cTnT-spiked PBS (as in Figure 6), indicating the specific detection of cTnI.

The present study has primarily displayed the current value changes upon molecular attachment or interaction either during surface modification or molecular assembly. The differences in the current value output support these

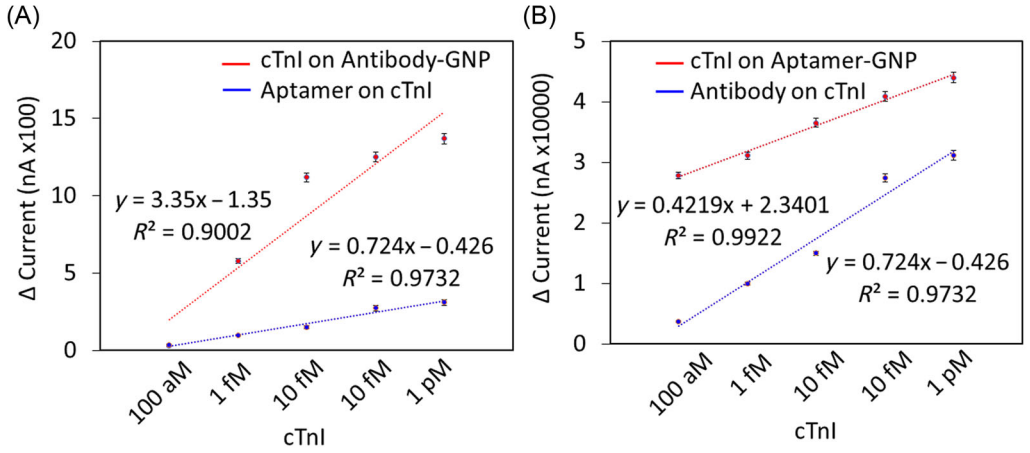

FIGURE 7 Comparison of the current difference for (A) cTnI on the antibody and aptamer on cTnI. (B) cTnI on the aptamer and antibody on cTnI. Linear regression analyses were performed, and the sensitivities were estimated by 3σ. Error bars are based on average values with replicates.

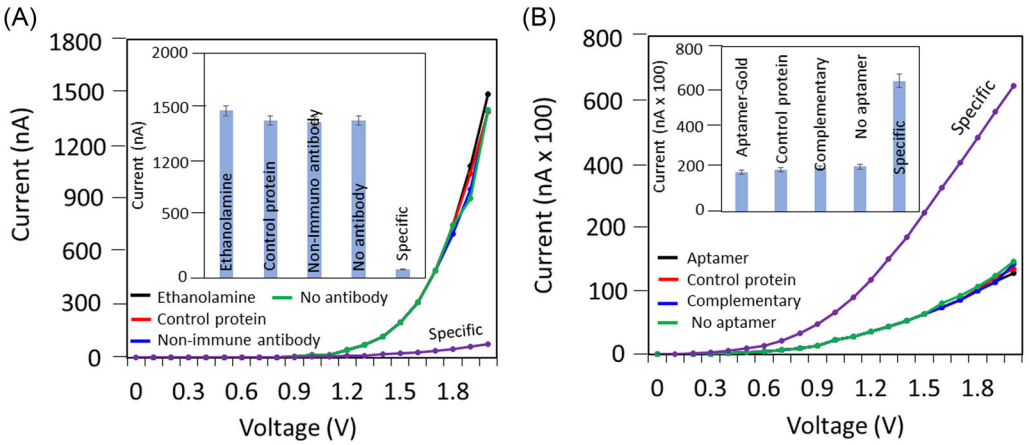

FIGURE 8 Control experiments for the specific detection of cTnI. (A) On the antibody surface. Nonimmune antibody instead of cTnI antibody, troponin T instead of cTnI, and no antibody were tested. (B) On the aptamer surface. Complementary instead of aptamer sequences, troponin T instead of cTnI, and no aptamer were tested. In both experiments, the control experiments did not show significant changes in current, indicating the specific detection of cTnI. Error bars are based on average values with replicates.

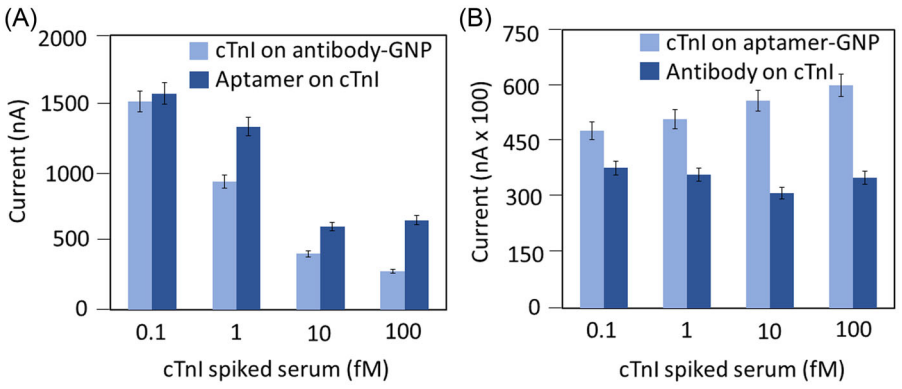

FIGURE 9 Specificity analysis in spiked serum. (A) Current changes by interacting cTnI with the antibody and aptamer. (B) Current changes by interacting cTnI with the aptamer and antibody. cTnI at different concentrations was spiked in 1:100 diluted serum. Error bars are based on average values with replicates.

surface changes and occur through the process or mechanism called the "dipole moment." These dipole moments are due to ionic movement or ionic exchange in the reaction media placed on the sensing surface. Since IDE has two electrodes (positive and negative) to recognize these alterations, there were current value changes measured by a picoammeter at the desired current ranges.[30,33]

4 | CONCLUSIONS

The incidence of CVD is increasing every year, affecting populations worldwide. According to the World Health Organization, the incidence of CVD is expected to increase more in the coming years. Among other CVD-related occurrences, MI is highly correlated with cardiac arrest and heart attack, leading to death and damage to other organs of the body. The current research is focused on detecting the cardiac biomarker troponin I (cTnI) and quantifying it on a metal oxide IDE surface by using antibody-cTnI-aptamer and aptamer-cTnI-antibody sandwich patterns. The LOD of cTnI was found to be 1 fM with the antibody and 100 aM with the aptamer. Moreover, the aptamer-cTnI-antibody sandwich pattern improved the current level at all cTnI concentrations tested. A higher specificity for cTnI was observed in the control experiments involving a complementary aptamer and discrimination against troponin T. The demonstrated strategies provide different options for developing sensing methods with dual probes.

ACKNOWLEDGMENTS

This project was supported by the Sichuan Medical Research Youth Innovation Program (Q15071) and Sichuan Medical Research Program (S15036) to Hu Hui.

ORCID

Hu hui https://orcid.org/0000-0002-8347-4687
Yeng Chen https://orcid.org/0000-0002-0064-7678
K. Pandian https://orcid.org/0000-0003-4130-9701

REFERENCES

1. Lee T, Ahn J-H, Choi J, Lee Y, Kim J-M, Park C, et al. Development of the troponin detection system based on the nanostructure. Micromachines. 2019;2019:203.
2. Rezaei B, Ghani M, Shoushtari AM, Rabiee M. Electrochemical biosensors based on nanofibres for cardiac biomarker detection: a comprehensive review. Biosens Bioelectron. 2016;2016:513–23.
3. Lee T, Kim J, Nam I, Lee Y, Kim HE, Sohn H, et al. Fabrication of troponin i biosensor composed of multi-functional dna structure/AU nanocrystal using electrochemical and localized surface plasmon resonance dual-detection method. Nanomaterials. 2019;9:1000.
4. Kazemi SH, Ghodsi E, Abdollahi S, Nadri S. Porous graphene oxide nanostructure as an excellent scaffold for label-free electrochemical biosensor: detection of cardiac troponin I. Mater Sci Eng, C. 2016;69:447–52.
5. Brancaccio P, Lippi G, Maffulli N. Biochemical markers of muscular damage. Clin Chem Lab Med. 2010:2010:757–67.
6. Kucherenko IS, Soldatkin OO, Lagarde F, Jaffrezic-Renault N, Dzyadevych SV, Soldatkin AP. Determination of total creatine kinase activity in blood serum using an amperometric biosensor based on glucose oxidase and hexokinase. Talanta. 2015;144:604–11.
7. Qureshi A, Gurbuz Y, Niazi JH. Biosensors for cardiac biomarkers detection: a review. Sensors Actuators, B Chem. 2012;171–172:62–76.
8. Yola ML, Atar N. Development of cardiac troponin-I biosensor based on boron nitride quantum dots including molecularly imprinted polymer. Biosens Bioelectron. 2019;126:418–24.
9. Tan CM, Arshad MKM, Fathil MFM, Adzhri R, et al., 2016. In: Proceedings of the IEEE International Conference on Semicondor Electronics (ICSE). Piscataway, NJ: IEEE. pp. 220–223.
10. Mcgill MR, Jaeschke H. Biomarkers of mitotoxicity after acute liver injury: further insights into the interpretation of glutamate dehydrogenase. J Clin Transl Res. 2021;7:61–65.
11. Liu Q, Ding JJ, Liu FY, Jiang ZZ, Li L, Xiao XB, et al. The novel biomarkers in diagnosis of prostate cancer. Cancer Plus. 2019;1:8–16.
12. Montano N, D'Alessandris QG, Izzo A, Fernandez E, Pallini R. Biomarkers for glioblastoma multiforme: status quo. J Clin Transl Res. 2016;2:3–10.
13. Yang Z, Zhang N, Shen Z, Bai S, Shi M, Yin L, et al. Markers for early diagnosis and post-operative recurrence monitoring of bladder cancer. Cancer Plus. 2020;2:43–52.
14. Wei Q, Nagi R, Sadeghi K, Feng S, Yan E, Ki SJ, et al. Detection and spatial mapping of mercury contamination in water samples using a smart-phone. ACS Nano. 2014;8:1121–9.
15. Gopinath SCB, Awazu K, Tominaga J, Kumar PKR. Monitoring biomolecular interactions on a digital versatile disk: a BioDVD platform technology. ACS Nano. 2008;2:1885–95.
16. Mi J, Liu Y, Rabbani ZN, Yang Z, Urban JH, Sullenger BA, et al. In vivo selection of tumor-targeting RNA motifs. Nat Chem Biol. 2010;6:22–24.
17. Liu D, Lu X, Yang Y, Zhai Y, Zhang J, Li L. A novel fluorescent aptasensor for the highly sensitive and selective detection of cardiac troponin I based on a graphene oxide platform. Anal Bioanal Chem. 2018;410:4285–91.
18. Hou Y, Wang W, Bartolo PJDS. Investigating the effect of carbon nanomaterials reinforcing poly(ε-caprolactone) scaffolds for bone repair applications. Int J Bioprint. 2020;6:1–9.
19. Rueda-Gensini L, Serna JA, Cifuentes J, Cruz JC, Muã±Oz-Camargo C. Graphene oxide-embedded extracellular matrix-derived hydrogel as a multiresponsive platform for 3D bioprinting applications. Int J Bioprint. 2021;7:1–16.
20. Carrasco-esteban E, Domínguez-rullán JA, Barrionuevo-castillo P, Pelari-mici L, López-campos F. Current role of nanoparticles in the treatment of lung cancer. J Clin Transl Res. 2021;7:140–55.
21. Zhang L, Li L. Colorimetric thrombin assay using aptamer-functionalized gold nanoparticles acting as a peroxidase mimetic. Microchim Acta. 2016;183:485–90.

22. Holzinger M, Goff AL, Cosnier S. Nanomaterials for biosensing applications : a review. 2014;2:1–10.
23. Koch L, Brandt O, Deiwick A, Chichkov B. Laser assisted bioprinting at different wavelengths and pulse durations with a metal dynamic release layer: a parametric study. Int J Bioprint. 2017;3:42–53.
24. Zhang Y, Attarilar S, Wang L, Lu W, Yang J, Fu Y. A review on design and mechanical properties of additively manufactured niti implants for orthopedic applications. Int J Bioprint. 2021;7:15–42.
25. Shuai C, Li Y, Yang W, Yu L, Yang Y, Peng S, et al. Graphene oxide induces ester bonds hydrolysis of poly-l-lactic acid scaffold to accelerate degradation. Int J Bioprint. 2020;6:91–104.
26. Weiss NO, Zhou H, Liao L, Liu Y, Jiang S, Huang Y, et al. Graphene: an emerging electronic material. Adv Mater. 2012;24:5782–825.
27. Wang J, Zhou HS. Colorimetric biosensor for food chemical hazards detection. In: Wang, S, editor, Food Chemical Hazard Detection: Development and Application of New Technologies. Oxford, UK: Wiley-Blackwell. 2014:291–313.
28. Chen S, Jang TS, Pan HM, Jung HD, et al. 3D freeform printing of nanocomposite hydrogels through in situ precipitation in reactive Viscous fluid. Int J Bioprint. 2020;6:1–21.
29. Jo H, Gu H, Jeon W, Youn H, Her J, Kim S-K, et al. Electrochemical aptasensor of cardiac troponin I for the early diagnosis of acute myocardial infarction. Anal Chem. 2015;87:9869–75.
30. Letchumanan I, Gopinath SCB, Md Arshad MK, Anbu P, Lakshmipriya T. Gold nano-urchin integrated label-free amperometric aptasensing human blood clotting factor IX: a prognosticative approach for “Royal disease”. Biosens Bioelectron. 2019;131:128–35.
31. Ramanathan S, Gopinath SCB, Md Arshad MK, Poopalan P, Loong FK, Lakshmipriya T, et al. Assorted micro-scale interdigitated aluminium electrode fabrication for insensitive electrolyte evaluation: zeolite nanoparticle-mediated micro- to nano-scaled electrodes. Appl Phys A. 2019;125:548.
32. Ong CC, Gopinath SCB, Rebecca LWX, Perumal V, Lakshmipriya T, Saheed MSM. Diagnosing human blood clotting deficiency. Int J Biol Macromol. 2018;116:765–73.
33. Ge Y, Lakshmipriya T, Gopinath SC, Anbu P, Chen Y, Hariri F, et al. Glucose oxidase complexed gold-graphene nanocomposite on a dielectric surface for glucose detection: a strategy for gestational diabetes mellitus. Int J Nanomed. 2019;14:7851–60.
34. Negahdary M, Behjati-Ardakani M, Sattarahmady N, Heli H. An aptamer-based biosensor for troponin I detection in diagnosis of myocardial infarction. J Biomed Phys Eng. 2018;8:167–78.
35. Lv Q, Wang Y, Su C, Lakshmipriya T, Gopinath SCB, Pandian K, et al. Human papilloma virus DNA-biomarker analysis for cervical cancer: signal enhancement by gold nanoparticle-coupled tetravalent streptavidin-biotin strategy. Int J Biol Macromol. 2019;134:354–60.

How to cite this article: hui H, Gopinath SCB, Ismail ZH, Chen Y, Pandian K, Velusamy P. Cardiovascular biomarker troponin I biosensor: Aptamer-gold-antibody hybrid on a metal oxide surface. Biotechnology and Applied Biochemistry. 2022;1–11. https://doi.org/10.1002/bab.2380